World Academy of Science, Engineering and Technology
International Journal of Mechanical and Mechatronics Engineering
Vol:16, No:9, 2022

Predictions and Comparisons of Thermohydrodynamic State for Single and Three Pads Gas Foil Bearings Operating at Steady-State Based on Multi-Physics Coupling Computer-Aided Engineering Simulations

Tai Yuan Yu, Pei-Jen Wang

***Abstract*—**Oil-free turbomachinery is considered one of the critical technologies for future green power generation systems as rotor machinery systems. Oil-free technology allows clean, compact, and maintenance-free working, and gas foil bearings (GFBs) are important for the technology. Since the first applications in the auxiliary power units and air cycle machines in the 1970s, obvious improvement has been created to the computational models for dynamic rotor behavior. However, many technical issues are still poorly understood or remain unsolved, and some of those are thermal management and the pattern of how pressure will be distributed in bearing clearance. This paper presents a three-dimensional (3D) fluid-structure interaction model of single pad foil bearings and three pad foil bearings to predict bearing working behavior that researchers could compare characteristics of those. The coupling analysis model involves dynamic working characteristics applied to all the gas film and mechanical structures. Therefore, the elastic deformation of foil structure and the hydrodynamic pressure of gas film can both be calculated by a finite element method program. As a result, the temperature distribution pattern could also be iteratively solved by coupling analysis. In conclusion, the working fluid state in a gas film of various pad forms of bearings working characteristic at constant rotational speed for both can be solved for comparisons with the experimental results.

***Keywords*—**Fluid structure interaction multi-physics simulations, gas foil bearing, oil-free, transient thermohydrodynamic.

I. Introduction

GAS foil bearings are one of the prospective bearings for environmentally-friendly rotor machinery system applications. There is a lot of research that has already been reported in some analytical models [1] and experimental results [2]-[7]. To improve the start and stop performance and apply it to large systems, hydrostatic bearings were also introduced [8]. Although many computational models are already built for the rotordynamic behavior of GFBs, some technical issues and operation characteristics still remain poorly understood or unsolved. Some of them are thermal management issues and pressure arrangement pattern of bearing. Even though the heat generated by bearing is low, limited heat dissipation ability, high speed working condition and unsuitable rotor system design could cause the thermal runaway or instability [9], [10]. Especially, when a bearing is operating in a high environment temperature such as near a turbine, those issues will be very critical, even involving heat transfer through the bearing housing, rotor, seals, etc. The instability issue of thermal is caused by uneven thermal heat transfer, unbalance between the heat dissipation characteristic of the components around the bearing. Therefore, the importance of the aerodynamics model of GFBs was put forward by many researchers, and several thermohydrodynamic (THD) models of GFBs were reported previously. Salehi et al. [11] presented a simplified model by using the Couette flow equation to simulate the thermal behavior of GFBs while predicting higher temperature than measurements. Peng and Khonsari [12] developed the first 3D THD simulation model for GFBs when the rotor assumed working in the mean temperature of the side leakage flow with simple thermal boundary conditions. However, their model did not include the detailed heat transfer behavior of the foil structure. San Andrés and Kim [13] developed two-dimensional (2D) THD model of GFBs by using Reynolds–Colburn analogy model to define the convection coefficients in different locations. Lee and Kim [14] presented a comprehensive 3D THD model of GFBs which considers the detailed thermal model for the channels of the bump foil. In that model, the bump foil structure is considered a heat exchanger, and the cooling gas along the axial direction and the temperature distribution of the bump foils are calculated by the thermal contact resistance between the bumps, top foil and bearing sleeve. The single and three pads GFBs with hydrodynamic preload [1], [8] have many special phenomena such as lower start up friction force and higher rotor stability compared with the continuous circular single pad GFBs. The schematics of the configuration of single and three pads GFBs are shown in Fig. 1.

Kim et al. [15] also presented the paper related to the thermal behavior of GFBs with single and three pads top foils. They predicted lower gas film temperature of the three pads GFBs compared with the single one under moderate loading of bearing. The improved thermal characteristics of the three pads

Tai Yuan Yu and Pei-Jen Wang are with the National Tsing Hua University, No. 101, Sec. 2, Guangfu Rd., East Dist., Hsinchu City., Taiwan R.O.C. (e-mail: www6112000@gmail.com, pjwang@pme.nthu.edu.tw).

GFBs are created by the shorter flow passage length of top foil along the circumferential direction of bearing. Simulation model presented by [14] and [15] also provides useful information about thermal transfer features during bearing operating below the load capacity.

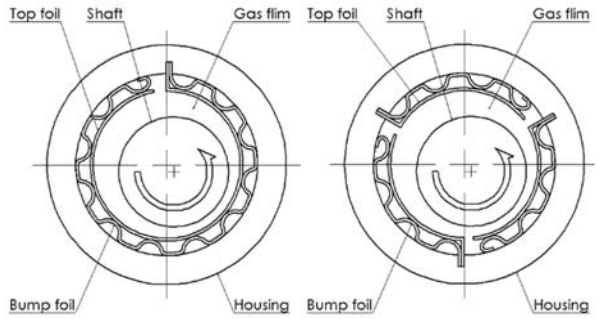

Fig. 1 2D schematics of bump-type GFB with single and three pads foil structure; main parts including bump foil, top foil, housing and shaft with circular arrow indicating the rotational direction

This paper provides a numerical simulation model for both single and three pads GFBs including all factors such as stiffness of bumps, interaction forces, friction forces between foils and local deformation of the top foil. Therefore, this simulation model would consider the effects of interaction forces and friction forces between the foils. A 3D commercial computer aided engineering (CAE) analysis program, copyrighted by Ansys Inc., USA, with built-in multi-physics coupling simulation capability could investigate the GFBs.

II. Numerical Simulation Analysis Model of Both Types of Gas Foil Bearing

Because the performance of GFB is decided by the interaction between each component around bearing, building the simulation model which could predict and simulate the working characteristic of GFB during operating is very important. However, the working fluid state of bearing will be directly affected by the shape of clearance between top foil and shaft surface. For the same reason, the foil surface will be reshaped by different working fluid states. This interaction relationship will never converge to a steady state. Therefore, establishing the simulation model of GFBs in the multi-physics field is necessary. In this study, GFBs model consists of transient structural and CFX modules which both include in commercial multi-physics program Ansys, copyrighted by Ansys Inc.

Initial and boundary conditions of thermal fluid and structure both can be set in this model individually and the result can be solved during the data exchange between different field interfaces to simulate the situation of GFBs operating with various pad forms. Meanwhile, time steps will be kept accumulating and create a complete process of GFBs.

Due to the fact that the property of GFBs was affected by the state of working fluid in the clearance directly, we create a computational fluid dynamics (CFD) model to specifically analyze the fluid state of GFBs for both single and three pads foil bearings. Most applications of GFBs working in certain stable boundary conditions like environment temperature, pressure or rotation speed can be directly set as the boundary conditions in back, front and inner surface of CFD model. After that, the heat transfer coefficient between the fluid field and structure can also be set on the outside surface, too. On the other hand, the structure model of GFBs like shaft and foil structure can also be built in the transient structure module of Ansys by using the similar method as the fluid field model. We set the bump foil as a homogeneous material structure and define the material properties of top foil and bump foil individually. This setting reduces the complexity of the analysis process effectively. It is worth noting that the model of foil structure should be arranged in a corresponding form to fit the different types of pads. For single pad and three pads foil bearings, see Figs. 2 and 3 for details.

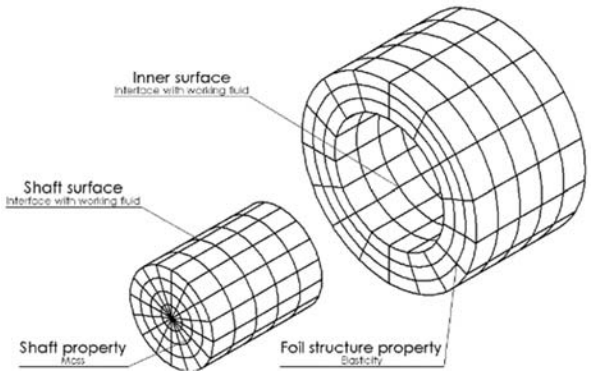

Fig. 2 Projective schematics of single pad foil structure and shaft in Transient Structure module

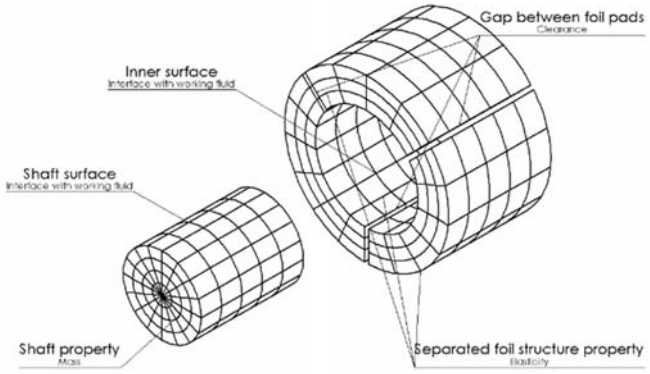

Fig. 3 Projective schematics of three pads foil structure and shaft in Transient Structure module

After we built the mechanical structure and fluid field simulation model of GFBs, the multi-physics coupling simulation could be achieved by the data transmission between each analysis model. Finally, the system coupling model can simulate the whole process bearing operating for both kinds of GFBs. For single pad and three pads foil bearings, see Figs. 4 and 5 for details.

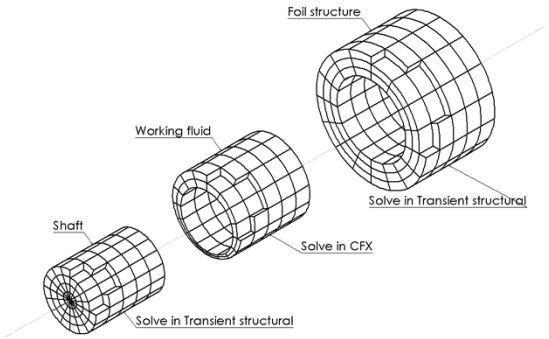

Fig. 4 Projective schematics including regions for of multi-domain coupling CAE simulations for single pad GFBs

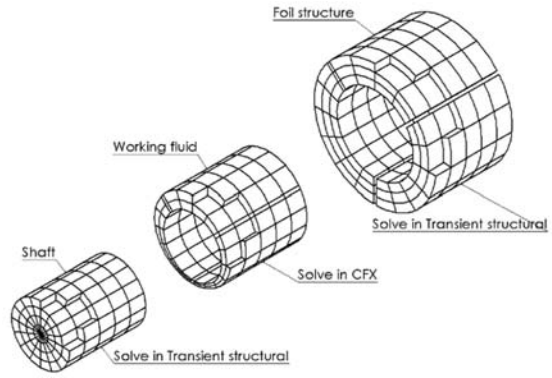

Fig. 5 Projective schematics including regions for of multi-domain coupling CAE simulations three pads GFBs

III. Results and Discussion

To simulate and compare the whole process of bearing working for different kinds of GFBs, we created a 3D geometry model to simulate the initial state of GFB within eccentricity is 0.8, which means to arrange a 38.1 mm (1.5 inch) diameter shaft in a hole with 50 mm average clearance for both simulation models. Therefore, the maximum and minimum thickness of clearance in the top and bottom side are 90 mm and 10 mm. See Fig. 6 for details for both single and three pads GFBs simulations model. On the other hand, the initial condition of mechanical structure and fluid field for both simulation models are also set in transient structure and CFX analysis module, see Table I for details.

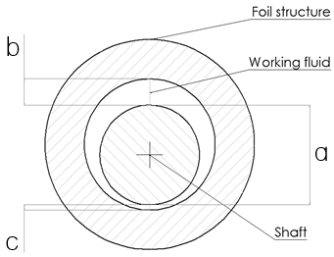

Fig. 6 Schematic to define the initial position for both single and three pads GFBs simulations model: a = 38.1 millimeter, b = 90 micrometer, c = 10 micrometer

TABLE I
Initial Condition of Analytical Model

Module	Factor	Value	Unit
CFX	Environment Pressure	1.0	Bar
CFX	Environment Temperature	303	K
CFX	Rotation Speed of shaft	6,000	rpm
CFX	Rotation Direction of shaft	Counterclockwise	NA
Transient Structural	Loading of shaft	1.0	N

After the multi-domain coupling analysis process completes, we can confirm the time-varying temperature and pressure arrangement pattern of working fluid. Therefore, we can know the state of working fluid property in each time interval when bearing is operating by checking those result data.

From Figs. 7-14, plots of contour maps presenting working fluid states about temperature and pressure of single pad GFBs are indicated when the shaft is at a different position as clock needle directions. On the other hand, From Figs. 15-22 are the similar plots series, but for three pads GFBs.

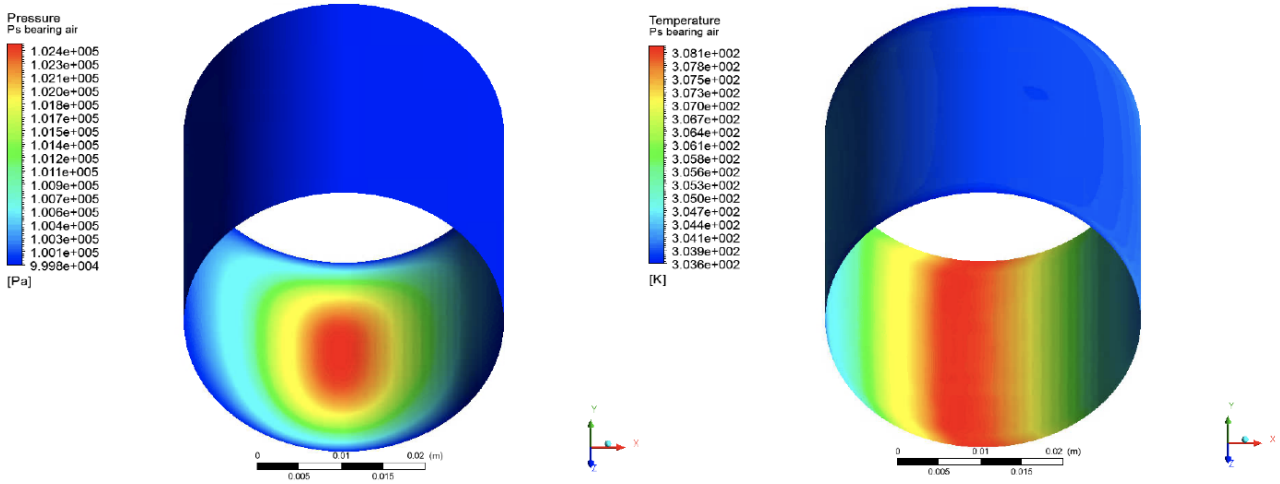

(a) (b)

Fig. 7 Plots of 3D contour map of working fluid states when the shaft being at 6 o'clock position of single pad GFBs: (a) figure of pressure arrangement and (b) figure of temperature arrangement

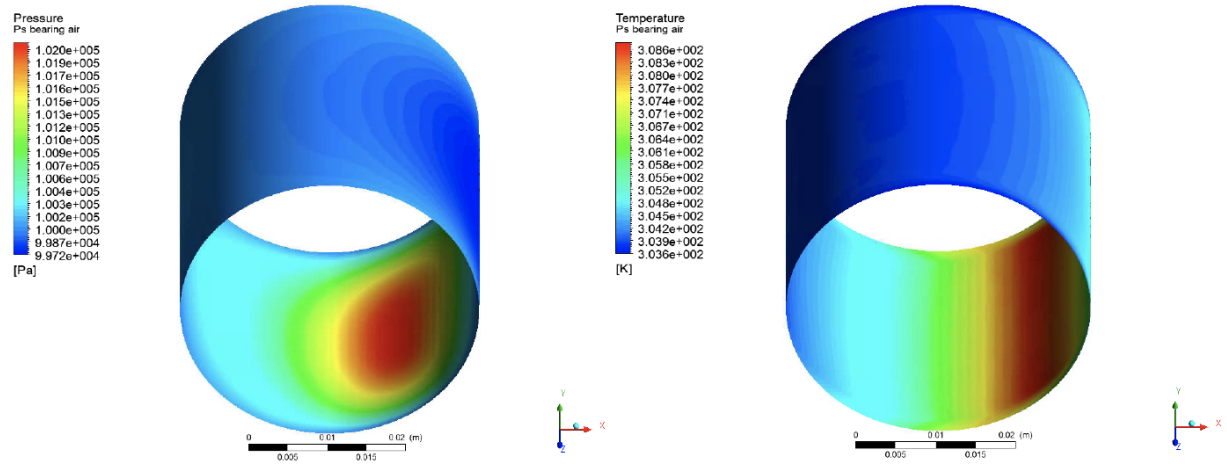

(a) (b)

Fig. 8 Plots of 3D contour map of working fluid states when the shaft being at 4.5 o'clock position of single pad GFBs: (a) figure of pressure arrangement and (b) figure of temperature arrangement

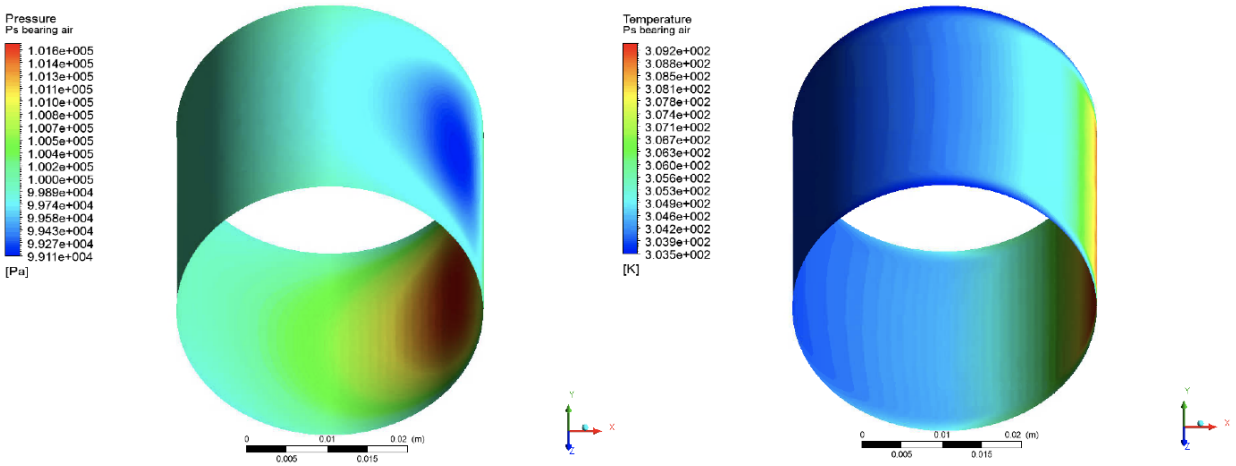

(a) (b)

Fig. 9 Plots of 3D contour map of working fluid states when the shaft being at 3 o'clock position of single pad GFBs: (a) figure of pressure arrangement and (b) figure of temperature arrangement

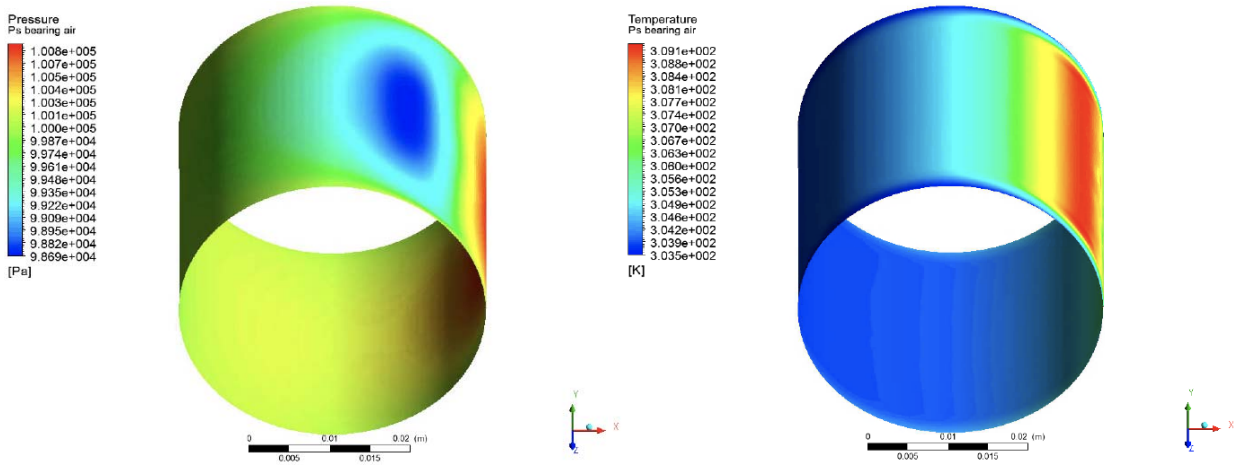

(a) (b)

Fig. 10 Plots of 3D contour map of working fluid states when the shaft being at 1.5 o'clock position of single pad GFBs: (a) figure of pressure arrangement and (b) figure of temperature arrangement

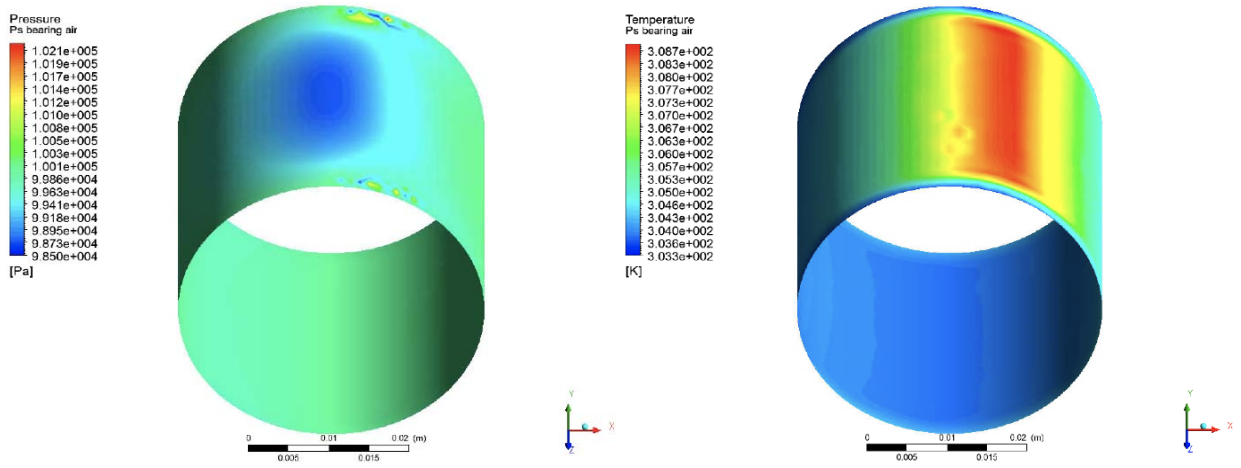

(a) (b)

Fig. 11 Plots of 3D contour map of working fluid states when the shaft being at 12 o'clock position of single pad GFBs: (a) figure of pressure arrangement and (b) figure of temperature arrangement

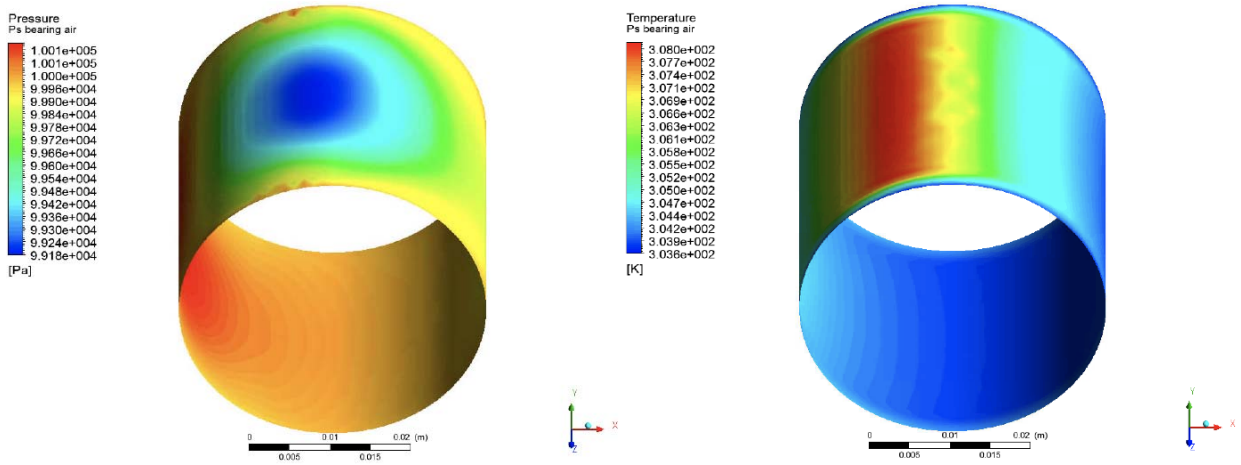

(a) (b)

Fig. 12 Plots of 3D contour map of working fluid states when the shaft being at 10.5 o'clock position of single pad GFBs: (a) figure of pressure arrangement and (b) figure of temperature arrangement

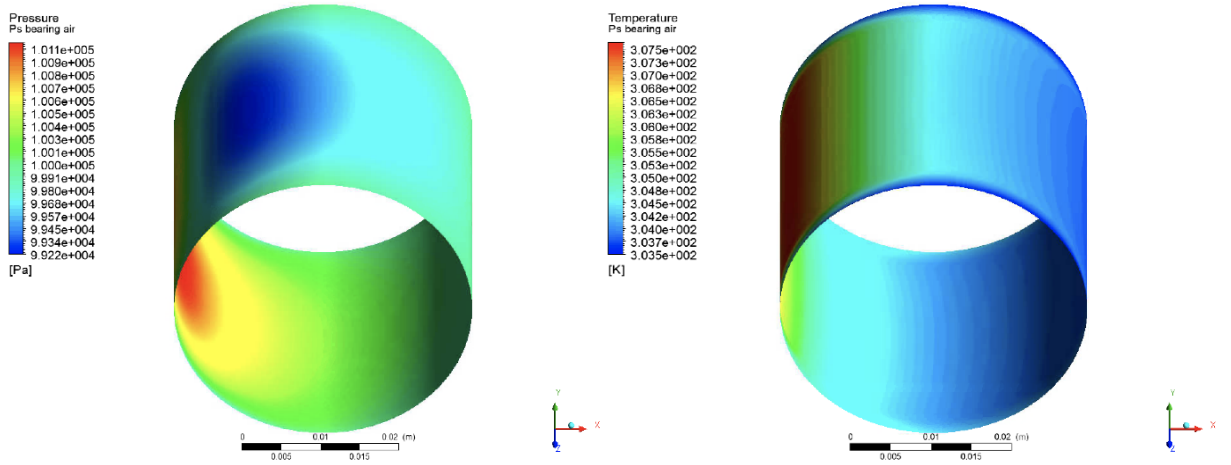

(a) (b)

Fig. 13 Plots of 3D contour map of working fluid states when the shaft being at 9 o'clock position of single pad GFBs: (a) figure of pressure arrangement and (b) figure of temperature arrangement

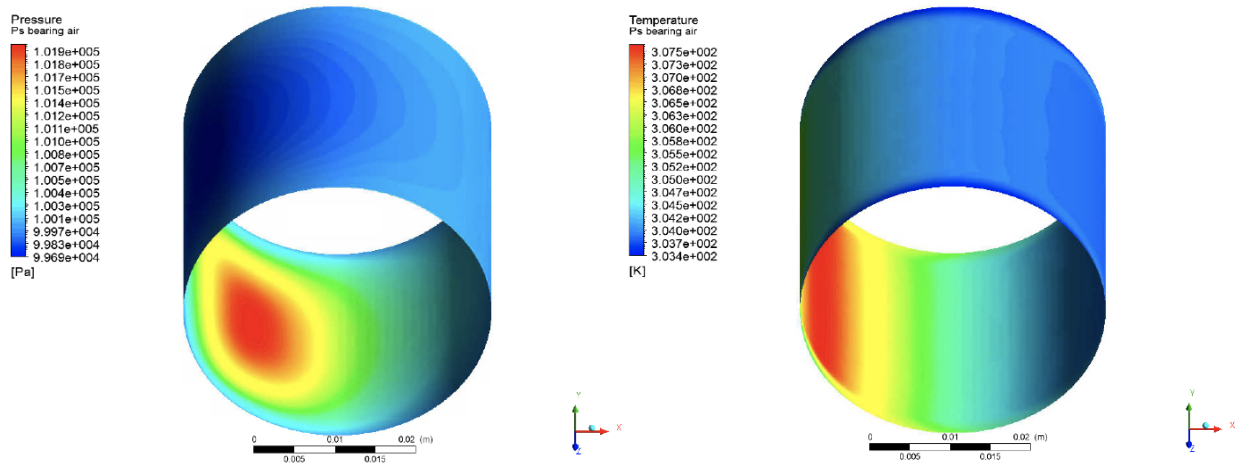

(a) (b)

Fig. 14 Plots of 3D contour map of working fluid states when the shaft being at 7.5 o'clock position of single pad GFBs: (a) figure of pressure arrangement and (b) figure of temperature arrangement

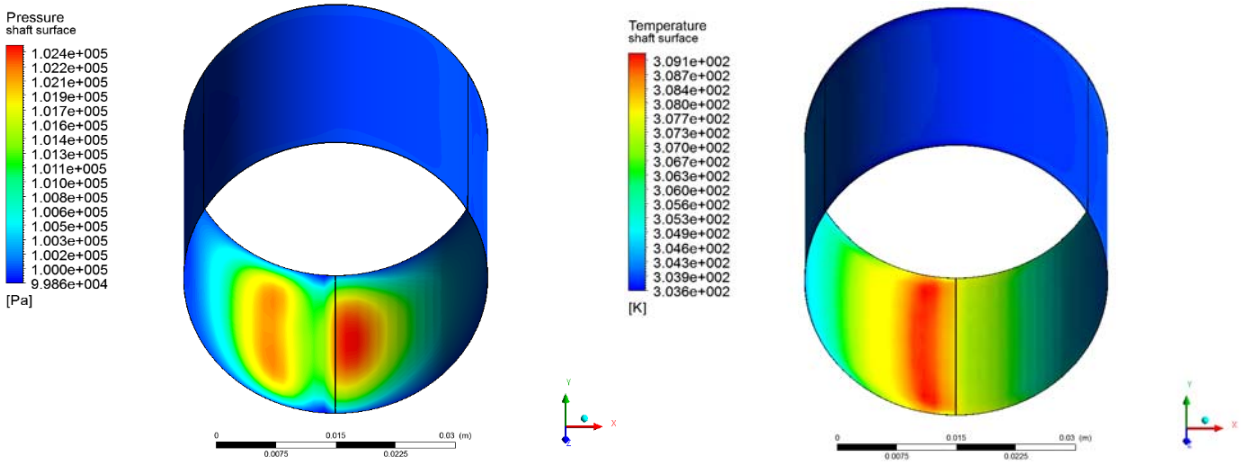

(a) (b)

Fig. 15 Plots of 3D contour map of working fluid states when the shaft being at 6 o'clock position of three pads GFBs: (a) figure of pressure arrangement and (b) figure of temperature arrangement

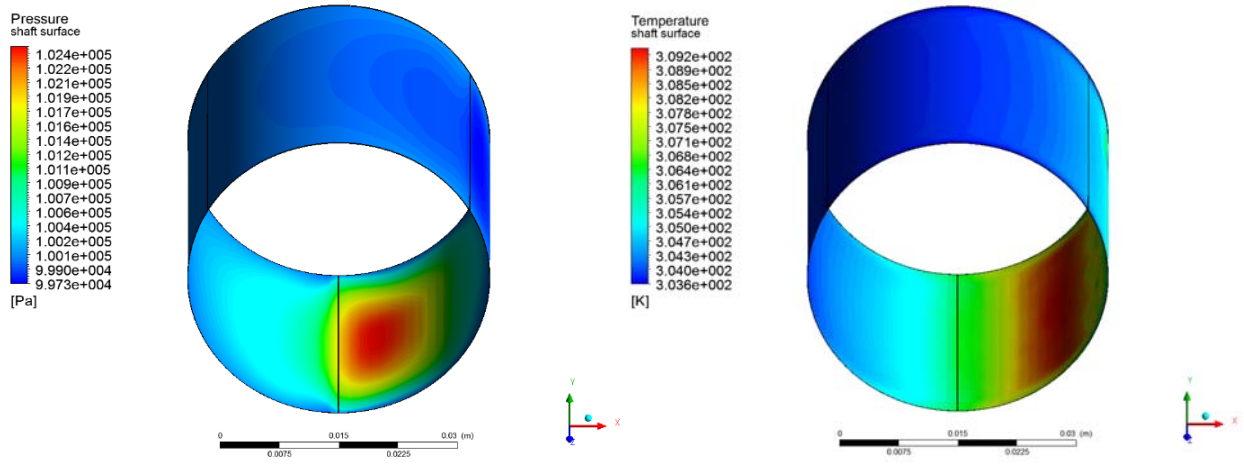

(a) (b)

Fig. 16 Plots of 3D contour map of working fluid states when the shaft being at 4.5 o'clock position of three pads GFBs: (a) figure of pressure arrangement and (b) figure of temperature arrangement

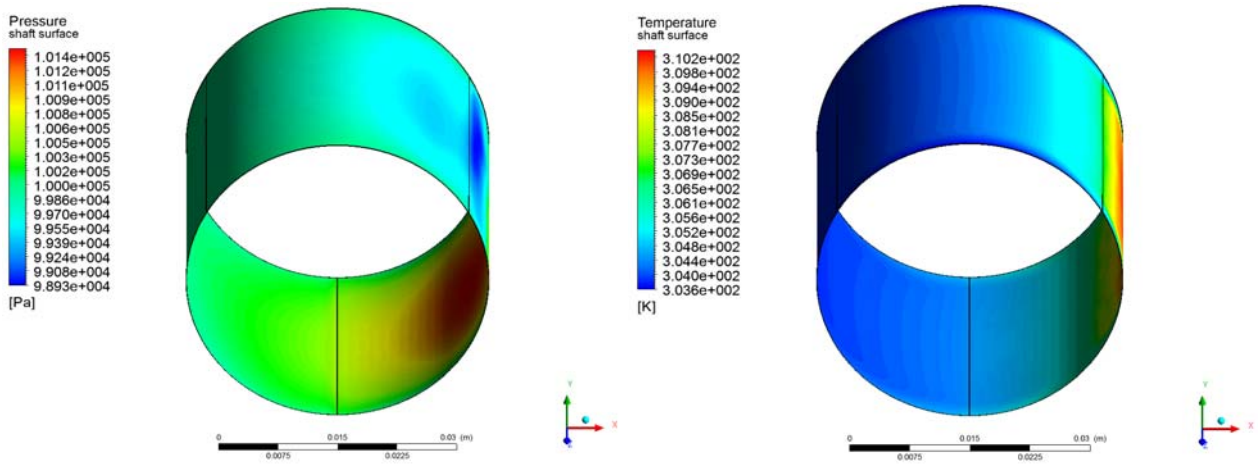

(a) (b)

Fig. 17 Plots of 3D contour map of working fluid states when the shaft being at 3 o'clock position of three pads GFBs: (a) figure of pressure arrangement and (b) figure of temperature arrangement

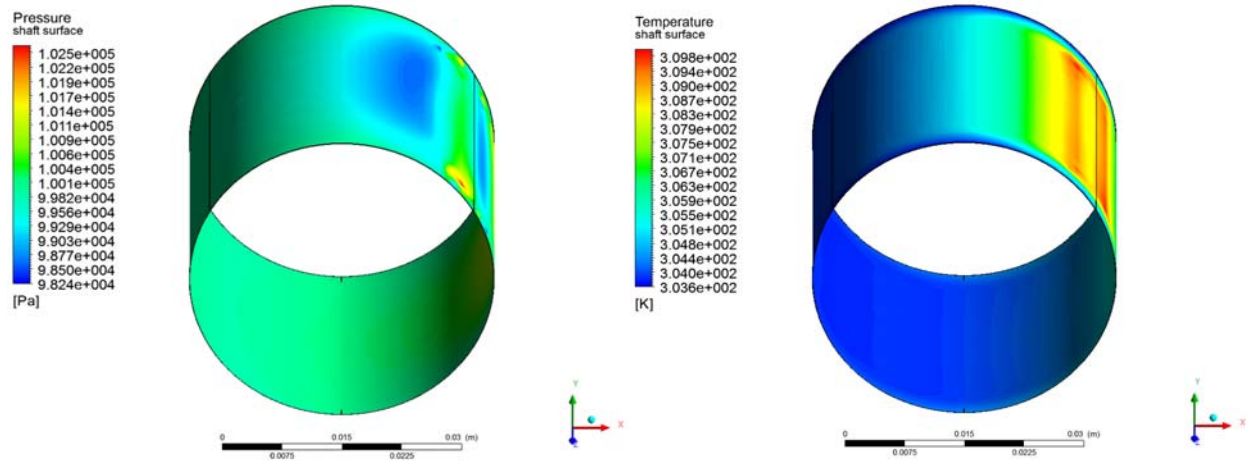

(a) (b)

Fig. 18 Plots of 3D contour map of working fluid states when the shaft being at 1.5 o'clock position of three pads GFBs: (a) figure of pressure arrangement and (b) figure of temperature arrangement

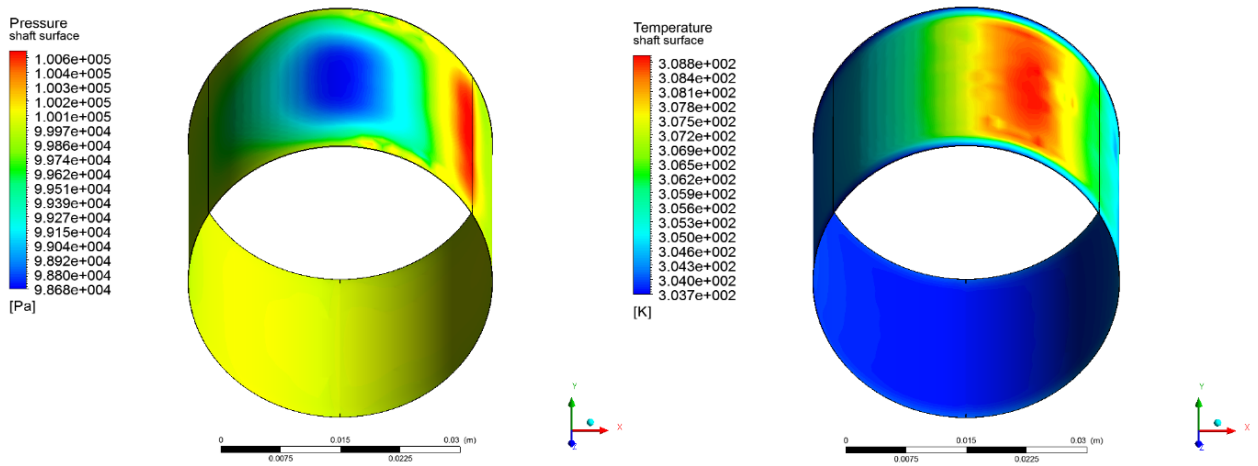

(a) (b)

Fig. 19 Plots of 3D contour map of working fluid states when the shaft being at 12 o'clock position of three pads GFBs: (a) figure of pressure arrangement and (b) figure of temperature arrangement

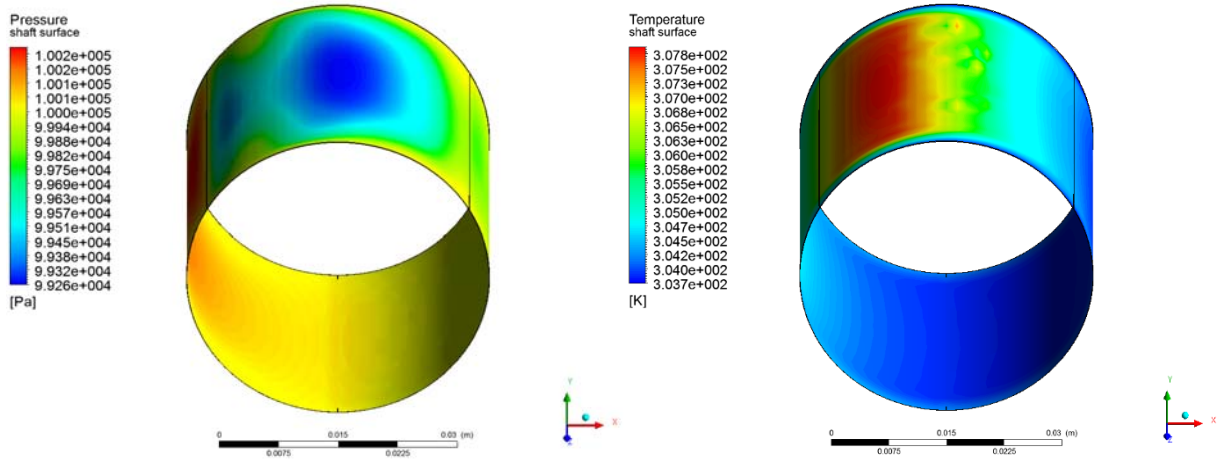

(a) (b)

Fig. 20 Plots of 3D contour map of working fluid states when the shaft being at 10.5 o'clock position of three pads GFBs: (a) figure of pressure arrangement and (b) figure of temperature arrangement

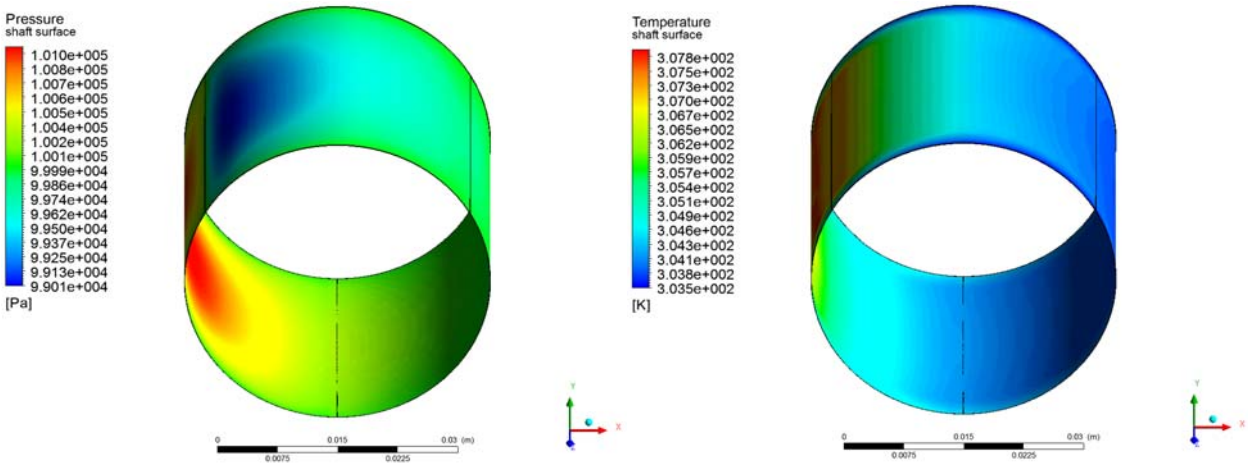

(a) (b)

Fig. 21 Plots of 3D contour map of working fluid states when the shaft being at 9 o'clock position of three pads GFBs: (a) figure of pressure arrangement and (b) figure of temperature arrangement

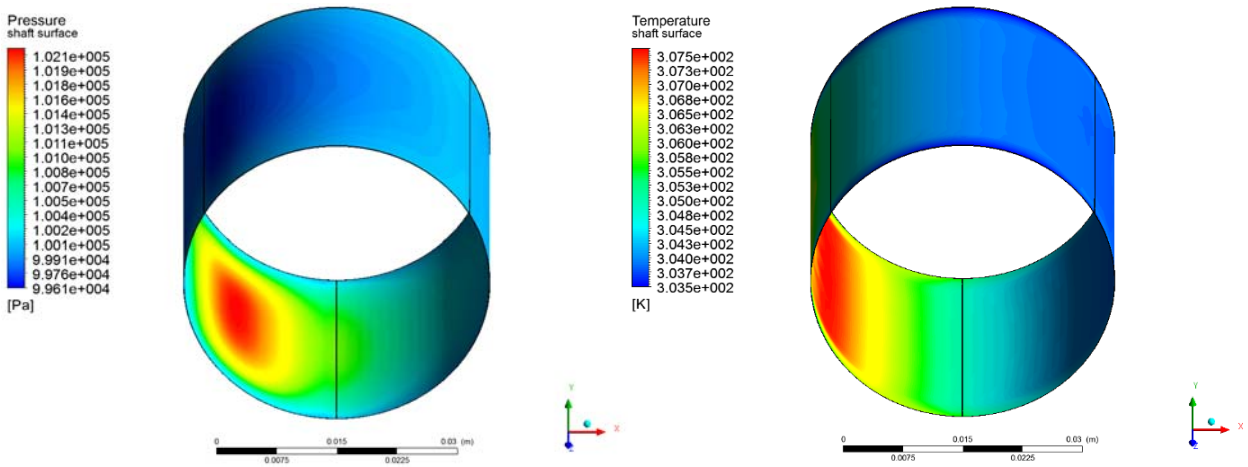

(a) (b)

Fig. 22 Plots of 3D contour map of working fluid states when the shaft being at 7.5 o'clock position of three pads GFBs: (a) figure of pressure arrangement and (b) figure of temperature arrangement

IV. Conclusion

The comparison of gas film characteristics including pressure and temperature of single and three pads GFBs is investigated in this paper. The simulation model is based on commercial multi-physics coupling CAE programs, copyrighted by Ansys Inc., USA. In the simulations, the effect of placing the single pad to three pads can be observed in temperature and pressure contour maps. The results indicate that the state of working fluid in clearance of GFB, like the pressure distribution state and temperature arrangement phenomena, can be affected by different kinds of foil structure selection directly. Those are both critical factors relative to bearing capacity such as stiffness, limit operating rotation speed and even required heat dissipation capacity.

Conclusively speaking, not only for single pad but also three-pad GFBs can be simulated by an analysis model built on a PC which is equipped with appropriate computation resources. The gap between each separated pads of foil structure can really create a space allowing the extra heat dissipation effect. However, it can make the pressure arrangement unsmooth too. Especially, the stress concentration phenomena in the edge of top foil can also be caused. The results of simulation can be used for experimental verifications published elsewhere in detailed information. It would be helpful when a designer is designing and selecting the GFBs in further work relative to rotor machinery design, even allowing experimental verifications and feature comparison on the working performances of GFBs.

References

[1] Kim, D., "Parametric Studies on Static and Dynamic Performance of Air Foil Bearings with Different Top Foil Geometries and Bump Stiffness Distributions," *ASME J. Tribol*., 129, (2007), pp. 354–364.

[2] Salehi, M., Heshmat, H., and Walton, J. F., "On the Frictional Damping Characterization of Compliant Bump Foils," *ASME J. Tribol.*, 125, (2003), pp. 804–813.

[3] Heshmat, H., "Advancements in the Performance of Aerodynamic Foil Journal Bearings: High Speed and Load Capacity," *ASME J. Tribol.*, 116, (1994), pp. 287–295.

[4] Heshmat, H., Walton, J. F., II, and Tomaszewski, M. J., "Demonstration of a Turbojet Engine Using an Air Foil Bearing," Turbo Expo 2005, *ASME Paper No. GT2005-68404*., (2005).

[5] DellaCorte, C., and Valco, M. J., 2000, "Load Capacity Estimation of Foil Air Journal Bearings for Oil-Free Turbo-Machinery Applications," *STLE Tribol. Trans*., 43, (2000), pp. 795–801.

[6] Howard, S. A., and DellaCorte, C., "Dynamic Stiffness and Damping Characteristics of a High-Temperature Air Foil Journal Bearing," *STLE Tribol. Trans*., 44, (2001), pp. 657–663.

[7] Radil, K., DellaCorte, C., and Zeszotek, M., "Thermal Management Techniques for Oil-Free Turbomachinery Systems," *STLE Tribol. Trans.*, 50, (2007), pp. 319–327.

[8] Kim, D., and Lee, D., "Design of Three-Pad Hybrid Air Foil Bearing and Experimental Investigation on Static Performance at Zero Running Speed," *ASME J. Eng. Gas Turbines Power*, 132, (2010), p. 122504.

[9] Dykas, B., and Howard, S. A., "Journal Design Considerations for Turbomachine Shafts Supported on Foil Air Bearings," *STLE Tribol. Trans*., 47, (2004), pp. 508–516.

[10] Radil, K., and Zeszotek, M., "An Experimental Investigation Into the Temperature Profile of a Compliant Foil Air Bearing," *STLE Tribol. Trans*., 47, (2004), pp. 470–479.

[11] Salehi, M., Swanson, E., and Heshmat, H., "Thermal Features of Compliant Foil Bearings—Theory and Experiments," *ASME J. Tribol*., 123, (2001), pp. 566–571.

[12] Peng, Z. C., and Khonsari, M., "A Thermohydrodynamic Analysis of Foil Journal Bearings," *ASME J. Tribol*., 128, (2006), pp. 534–541.

[13] San Andrés, L., and Kim, T. H., "Thermohydrodynamic Analysis of Bump Type Gas Foil Bearings: A Model Anchored to Test Data," Turbo Expo 2009, *ASME Paper No. GT2009-59919*., (2009).

[14] Lee, D., and Kim, D., "Thermo-Hydrodynamic Analyses of Bump Air Foil Bearings with Detailed Thermal Model of Foil Structures and Rotor," *ASME J. Tribol*., 132, (2010), p. 021704.

[15] Kim, D., Lee, D., Kim, Y. C., and Ahn, K. Y., "Comparison of Thermo-Hydrodynamic Characteristics of Airfoil Bearings With Different Top Foil Geometries," Proceedings of the Eighth IFToMM International Conference on Rotordynamics, Seoul, Korea, Sept. 12–15., (2010).